CHEMMEDCHEM

DOI: 10.1002/cmdc.201100511

3-Substituted 2-Phenylimidazo[2,1-*b*]benzothiazoles: Synthesis, Anticancer Activity, and Inhibition of Tubulin Polymerization

Ahmed Kamal,*[a, c] Farheen Sultana,[a] M. Janaki Ramaiah,[b] Y. V. V. Srikanth,[a] A. Viswanath,[a] Chandan Kishor,[b] Pranjal Sharma,[b] S. N. C. V. L. Pushpavalli,[b] Anthony Addlagatta,*[b] and Manika Pal-Bhadra*[b]

A new series of 3-substituted 2-phenylimidazo[2,1-*b*]benzothiazoles (**3a**–**h**) were synthesized by C-arylation of 2-arylimidazo-[2,1-*b*]benzothiazoles using palladium acetate as catalyst, and the resulting compounds were evaluated for their anticancer activity. Compounds **3a**, **3e**, and **3h** exhibited good antiproliferative activity, with GI_{50} values in the range of 0.19–83.1 μM. Compound **3h** showed potent anticancer efficacy against 60 human cancer cell lines, with a mean GI_{50} value of 0.88 μM. This compound also induced cell-cycle arrest in the G_2/M phase and inhibited tubulin polymerization followed by activation of caspase-3 and apoptosis. A high-throughput tubulin polymerization assay showed that the level of inhibition for compound **3h** is similar to that of combretastatin A-4. Molecular modeling studies provided a molecular basis for the favorable binding of compounds **3a**, **3e**, and **3h** to the colchicine binding pocket of tubulin.

Introduction

Microtubules are composed of dynamic polymers of tubulin that are involved in cellular processes and play an essential role in mitosis, especially in induction of apoptosis,[1] thus making them an important target in the development of compounds for the treatment of cancer.[2] Cells that divide rapidly have impaired microtubule dynamics, and are thus more susceptible to tubulin polymerization inhibitors and subsequent arrest during mitosis than non-dividing cells.[1] The hallmark of microtubule-interfering drugs is mitotic arrest, which ultimately leads to apoptosis.[3] Tubulin polymerization inhibitors specifically bind to any one of the three reported binding sites,[4] thereby stabilizing or destabilizing microtubule assembly.[5] Disruption of microtubule formation leads to cell-cycle arrest in the G_2/M phase, followed by apoptotic cell death.[4] Combretastatin A-4 (CA-4), a naturally occurring compound isolated from *Combretum caffrum*, binds to the colchicine binding site and exhibits potent anticancer activity against a wide variety of human cancer cell lines, including MDR cancer cell lines which possess tubulin polymerization-inhibiting properties.[6,7] Combretastatin A-4 phosphate (CA-4P), a prodrug of CA-4 is presently undergoing clinical trials as a tumor vasculature-targeting agent.[7–9] A number of CA-4 derivatives, containing five-membered heterocycles that are considered good surrogates for the CA-4 double bond as they retain the *cis*-alkene configuration, have been reported as potent tubulin inhibitors that exhibit enhanced cytotoxicity.[10]

Imidazoles are common scaffolds in highly significant biomolecules such as biotin, histamine, and in a number of alkaloids that exhibit a broad spectrum of biological properties including antimicrobial,[11] anticonvulsant,[12] sodium channel blocking,[13] anti-inflammatory,[14] CB1 receptor inverse agonist,[15] and anticancer activities.[16–18] In various imidazole-based compounds, the position of a substituent has been observed to have a significant effect on the mode of action. Various 1,5- and 1,2-diarylimidazoles exhibit anticancer activity through inhibition of COX-2.[19–21] Similarly, CA-4-based compounds such as 4,5-diaryl-1*H*-imidazole (**1**) (Figure 1) and 2-aryl-4-benzoylimidazoles exhibit anticancer activity through inhibition of tubulin polymerization.[22–24]

Benzothiazole, with its simple heterocyclic scaffold, has recently emerged as an important pharmacophore with potential anticancer activity.[25–29] Moreover, structural modification of the benzothiazole scaffold results in a variety of biological properties including antimicrobial,[30] anti-inflammatory,[31] immunosuppressive,[32] antiallergenic,[33] and anticancer activities.[34,35] 2-Arylimidazo[2,1-*b*][1,3]benzothiazole derivative YM-201627 (**2**), for example, is a fused imidazobenzothiazole compound that has shown potent anticancer activity against a number of solid

[a] *Dr. A. Kamal, F. Sultana, Dr. Y. V. V. Srikanth, A. Viswanath*
Division of Organic Chemistry
Indian Institute of Chemical Technology, Hyderabad 500607 (India)
E-mail: ahmedkamal@iict.res.in

[b] *Dr. M. J. Ramaiah, C. Kishor, P. Sharma, Dr. S. N. C. V. L. Pushpavalli, Dr. A. Addlagatta, Dr. M. Pal-Bhadra*
Chemical Biology Laboratory
Indian Institute of Chemical Technology, Hyderabad 500607 (India)
E-mail: manika@iict.res.in
anthony@iict.res.in

[c] *Dr. A. Kamal*
Catalytic Chemistry Chair, Chemistry Department
College of Science, King Saud University, Riyadh (Saudi Arabia)

Supporting information for this article is available on the WWW under http://dx.doi.org/10.1002/cmdc.201100511.

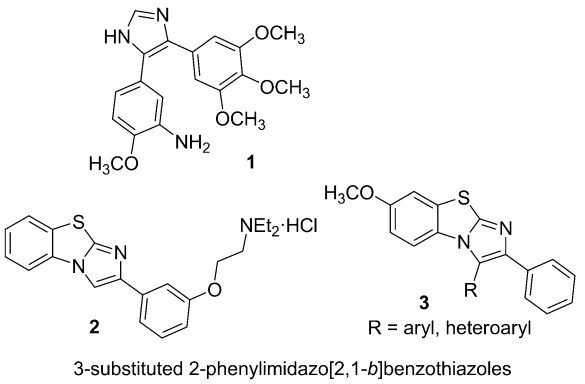

Figure 1. 4,5-diaryl-1*H*-imidazole (**1**), YM-201627 (**2**), and 3-substituted 2-phenylimidazo[2,1-*b*]benzothiazoles (**3**).

tumors and is considered useful in the treatment of cancer,[36] as well as being reported as an amyloid binding agent.[37] Other imidazo[2,1-*b*]benzothiazole derivatives have been identified as p53 inhibitors.[38] Recently, a new series of Mannich bases of 2-arylimidazo[2,1-*b*]benzothiazoles have been shown to possess anticancer activity, with the ability to induce apoptosis through inhibition of tubulin polymerization.[39]

Our earlier efforts toward the synthesis of a variety of novel molecules led to the development of efficient anticancer agents.[40–44] In the present investigation, an attempt has been made, in view of the biological importance of both diarylimidazoles and imidazobenzothiazole, to synthesize 3-substituted 2-phenylimidazo[2,1-*b*]benzothiazoles (**3**) using palladium-catalyzed arylation and heteroarylation of 2-arylimidazo[2,1-*b*]benzothiazoles. These compounds were evaluated for in vitro anticancer activity, cell-cycle effects, and potential to inhibit tubulin polymerization.

Results and Discussion

Chemistry

3-Substituted 2-phenylimidazo[2,1-*b*]benzothiazoles **3a**–**h** were prepared as shown in Scheme 1. Condensation of 6-methoxy-2-aminobenzothiazole (**4**) with 2-bromoacetophenone (**5**) in ethanol under reflux conditions for 1 h provided 7-methoxy-2-phenyl imidazo[2,1-*b*]benzothiazole (**6**). Upon C-arylation[45] with aryl and heteroaryliodo compounds **7a**–**h** in the presence of palladium acetate, copper iodide, and triphenyl phosphine, using cesium carbonate as a base and 1,4-dioxane as a solvent, afforded the desired benzothiazoles **3a**–**h** after 16 h at reflux.

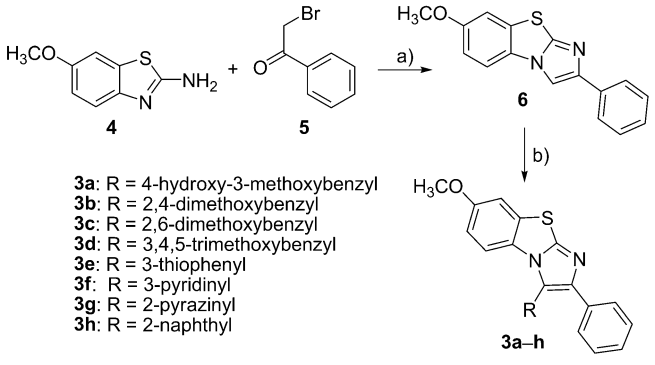

Scheme 1. *Reagents and conditions*: a) EtOH, reflux, 6–8 h, 65–80%; b) $Pd(OAc)_2$, CuI, PPh_3, aryl/heteroaryliodo compounds **7a**–**h**, Cs_2CO_3, 1,4-dioxane, reflux, 16 h, 74–88%.

Biological activity

Anticancer activity

Fused benzothiazoles **3a**–**h** were evaluated with regard to anticancer activity against 60 cancer cell lines derived from nine types of human cancer (lung, leukemia, colon, melanoma, ovarian, renal, prostate, and breast cancer) at the National Cancer Institute (NCI, Bethesda, MD, USA). Results are expressed as a percentage of growth inhibition (GI_{50}) determined relative to that of untreated control cells (Table 1). Among the eight benzothiazoles synthesized, three were active in the primary screen and were further evaluated against a panel of 60 cell lines at five concentrations, with results as shown in Table 2. These three compounds, **3a**, **3e**, and **3h**, exhibited a wide spectrum of activity against various cancer cell lines with mean GI_{50} values of 21.8, 5.12, and 0.88 μM, respectively. Specifically, compound **3h** exhibited excellent anticancer activity against sixty cancer cell lines, with GI_{50} values ranging from 0.19–3.30 μM. Compound **3e** also showed promising anticancer activity, particularly against MDA-MB-435 cell line (GI_{50} value of 0.32 μM). Compound **3a** exhibited anticancer activity in the micromolar range against certain cell lines tested. In this investigation, the phenyl ring remained unchanged while modifying the aryl/heteroaryl substitution of the imidazobenzothiazole ring system in an attempt to understand the SAR. It was observed that compounds having 2-naphthyl and 3-thienyl groups were the most active among the series. In contrast, aryl rings with electron-donating substituents and heteroaromatic groups such as 3-pyridyl and 2-pyrazinyl in the imidazobenzothiazole system (**3b**–**d** and **3f**–**g**) displayed lower activity in a majority of the cell lines. However, compound **3a**, with a 4-hydroxy-3-methoxyphenyl group, exhibited moderate anticancer activity with GI_{50} values ranging from 1.4 to 83.1 μM.

Table 1. Growth inhibition for selected cancer cell lines by 3-substituted 2-phenylimidazo[2,1-*b*]benzothiazoles.

Compound	Cell line	Inhibition [%][a]
3b (NSC 755298)	K-562	53.21
	MDA-MB-435	84.92
3d (NSC 755297)	HCT-116	51.81
	MDA-MB-435	86.37
3f (NSC 755303)	NCI-H522	−22.74[b]

[a] Determined at 10 μM; data were obtained from the NCI in vitro disease-oriented human tumor cell screen. [b] Negative value indicates cell death.

Table 2. Anticancer activity of 3-substituted 2-phenylimidazo[2,1-*b*]benzothiazole derivatives in human cancer cell lines.

Cancer Panel/cell line	GI_{50} [μM][a] **3a**[b]	**3e**[c]	**3h**[d]	Cancer Panel/cell line	GI_{50} [μM][a] **3a**[b]	**3e**[c]	**3h**[d]
Leukemia				*Ovarian*			
CCRF-CEM	NT[e]	NT[e]	0.45	IGROV1	>100	6.53	2.04
HL-60(TB)	5.33	3.90	0.26	OVCAR-3	10.1	2.15	0.37
K-562	4.53	0.87	0.38	OVCAR-4	39.1	3.71	3.10
MOLT-4	12.8	4.20	0.93	OVCAR-5	33.7	4.49	2.10
RPMI-8226	NT[e]	NT[e]	0.99	OVCAR-8	41.2	5.95	0.92
SR	3.34	2.02	0.35	NCI/ADR-RES	4.5	2.53	0.51
				SK-OV-3	19.6	3.48	0.28
Non-small-cell lung				*Renal*			
A549/ATCC	9.91	5.02	0.81	786-0	30.9	7.58	0.89
EKVX	74.7	7.76	3.30	A498	28.3	6.26	0.46
HOP-62	37.8	7.86	0.29	ACHN	38.9	6.76	0.84
HOP-92	28.0	9.89	NT[e]	CAKI-1	8.54	5.04	0.79
NCI-H226	22.05	2.17	0.50	RXF 393	4.9	1.66	0.18
NCI-H23	95.5	4.0	0.95	SN12C	80.5	12.1	0.68
NCI-H322M	>100	>100	5.17	TK-10	>100	37.7	3.00
NCI-H460	6.50	4.40	0.35	UO-31	81.0	6.03	1.80
NCI-H522	15.0	2.90	0.43				
Colon				*Breast*			
COLO 205	5.30	2.20	0.25	MCF7	28.6	3.78	0.35
HCC-2998	>100	4.80	1.50	MDA-MB-231	9.8	5.46	1.10
HCT-116	4.90	4.18	0.62	HS 578T	>100	>100	0.48
HCT-15	4.03	2.91	0.46	BT-549	17.5	6.55	1.80
HT29	3.56	2.95	0.33	T-47D	83.1	6.27	1.40
KM12	4.81	3.70	0.39	MDA-MB-468	24.3	1.98	1.10
SW-620	5.14	3.84	0.31				
CNS				*Prostate*			
SF-268	28.8	8.54	0.82	PC-3	26.3	4.02	0.50
SF-295	8.00	3.06	0.50	DU-145	35.4	3.45	0.80
SF-539	6.60	2.62	0.36				
SNB-19	32.5	6.90	0.64				
SNB-75	11.1	2.2	0.20				
U251	5.28	3.72	0.40				
Melanoma				*Melanoma*			
LOX IMVI	7.6	5.25	0.58	SK-MEL-28	8.9	4.90	0.41
MALME-3M	>100	>100	>100	SK-MEL-5	3.6	3.34	0.20
M14	4.3	2.64	0.55	UACC-257	>100	>100	0.49
MDA-MB-435	1.4	0.32	0.19	UACC-62	8.2	3.52	0.39
SK-MEL-2	21.3	9.72	0.35				

[a] Compound concentration required to decrease cell growth to half that of untreated cells. [b] **3a** (NSC 755302). [c] **3e** (NSC 755308). [d] **3h** (NSC 755307). [e] Not tested.

In vitro cytotoxicity

To understand the cytotoxic nature of these compounds, an MTT cytotoxicity assay was performed by treating A549 human lung cancer cell line with compounds **3a**–**h** at 4 μM for 24 h. It was observed that compounds **3e** and **3h** were found to cause significant cytotoxicity in cancer cells. Interestingly, compound **3h** showed cytotoxicity similar to that of CA-4, which was employed as a positive control in this assay (Figure 2).

Effect on cell cycle

Flow cytometry analysis was performed to investigate the mechanism of cell death. A549 cells were treated with 4 μM of **3a**–**h**, using CA-4 as the positive control, for 24 h. Compounds **3a**–**g** caused G1 phase cell-cycle arrest, while compound **3h** surprisingly caused G_2/M cell-cycle arrest with a large accumulation of cells (69%) in the G_2/M phase. Similar effects were observed for CA-4-treated cells (65%), as shown in Figure 3A. Furthermore, apoptosis-inducing ability was also observed for these compounds (**3e**, **3h**, and CA-4) with an increase in the percentage of cells in the G0 phase (Figure 3B).

Effect on inhibition of tubulin polymerization

Compounds that alter cell-cycle parameters with preferential G_2/M blockade are known to exhibit effects on tubulin assembly. Moreover, inhibition of tubulin polymerization is strongly associated with G_2/M cell-cycle arrest.[46] As compound **3h** ex-

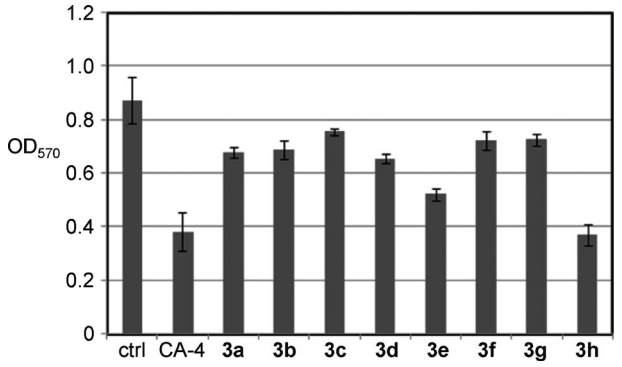

Figure 2. A549 cell viability observed by MTT assay following treatment with compounds **3a**–**h** for 24 h at 4 μM; 10000 cells per well were seeded in 96-well plates. CA-4 was used as a positive control; negative control (ctrl): DMSO alone without test compound. Error bars represent SD from the mean of triplicate measurements.

hibited G_2/M cell-cycle arrest, it was considered of interest to understand the microtubule inhibitory role of this compound. Therefore, A549 cells were treated with **3h**, CA-4, nocodozole (noc, a known tubulin inhibitor), and paclitaxel (pac, a known tubulin stabilizer) at 4 μM for 24 h. Compound **3h** resulted in dispersed microtubule organization relative to control cells, as observed by immunofluorescence and microscopy studies using anti α-tubulin antibody (Figure 4A).

Moreover, these results confirmed the transient transfection of tubulin–GFP-expressing plasmid in A549 cells following treatment with compounds **3h**, CA-4, and noc, whereas compound **3h** exhibited an inhibitory effect on tubulin polymerization (Figure 4B). We were therefore interested in investigating the level of tubulin inhibition for this compound (**3h**), for which we employed a high-throughput tubulin polymerization assay. Interestingly, **3h** demonstrated tubulin inhibition similar to that of CA-4. Pac was used as a tubulin polymerization stabilizer control (Figure 4C).

Activation of caspases

From previous reports, it is well established that molecules affecting microtubule polymerization cause mitotic arrest and ultimately lead to apoptosis.[47] It is also known that caspases play a vital and active role for the initiation and execution of the apoptotic process.[48] Among the caspases, caspase-3 is one of the key effector caspases which cleave multiple proteins in cells, leading to apoptotic cell death.[49] In this context, the effect of these conjugates in causing effective apoptosis in A549 cells was examined. Cells were treated with **3h**, CA-4, noc, and pac at 4 μM, and cell lysates were subjected to Western blot analysis. Results indicated that increased expression of active caspase-3 protein corresponds to the cell death-inducing nature of fused benzothiazole **3h**, as shown in Figure 5.

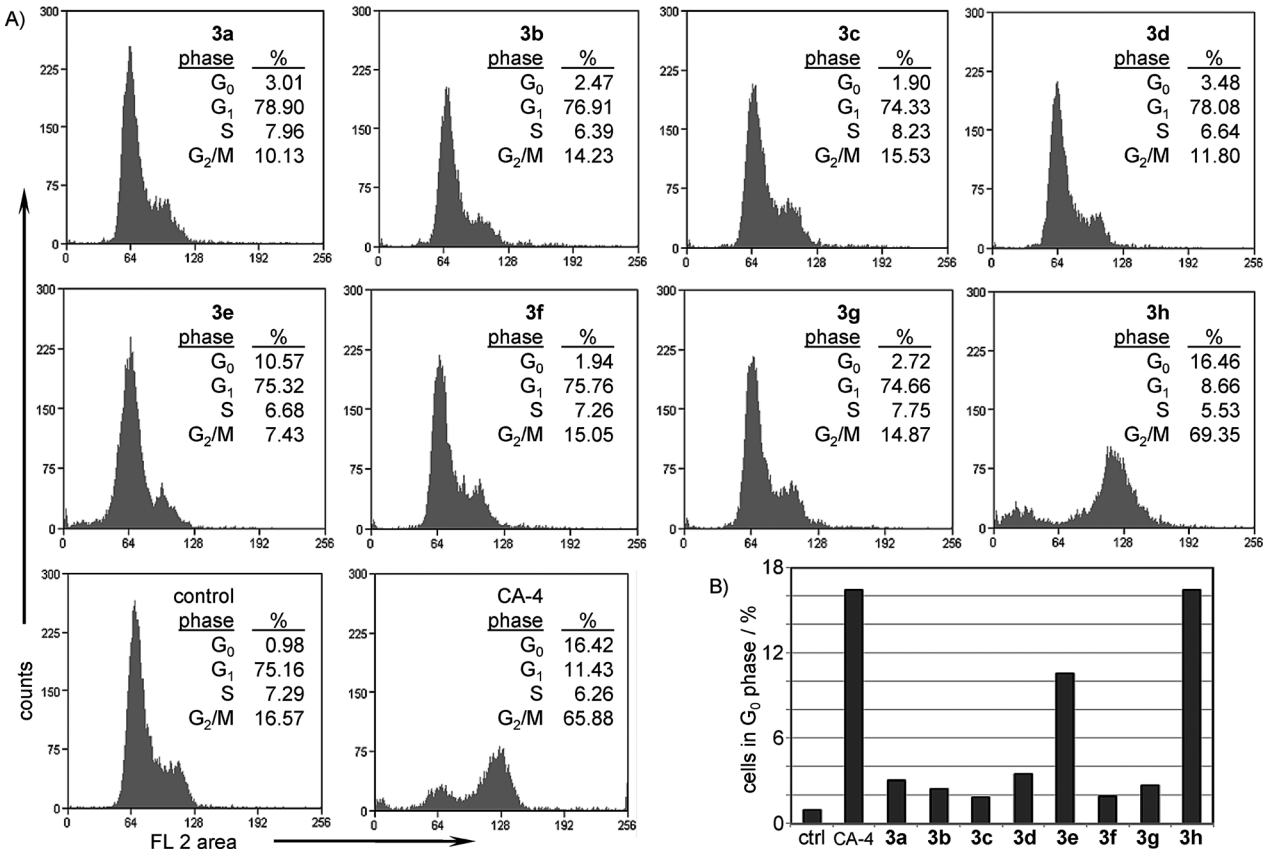

Figure 3. A) Effect of 3-substituted 2-phenylimidazo[2,1-*b*]benzothiazoles on cell cycle. A549 cells were treated with compounds **3a**–**h** at 4 μM for 24 h. CA-4 was used as positive control. B) Percent apoptosis following treatment with compounds **3a**–**h** at 4 μM for 24 h.

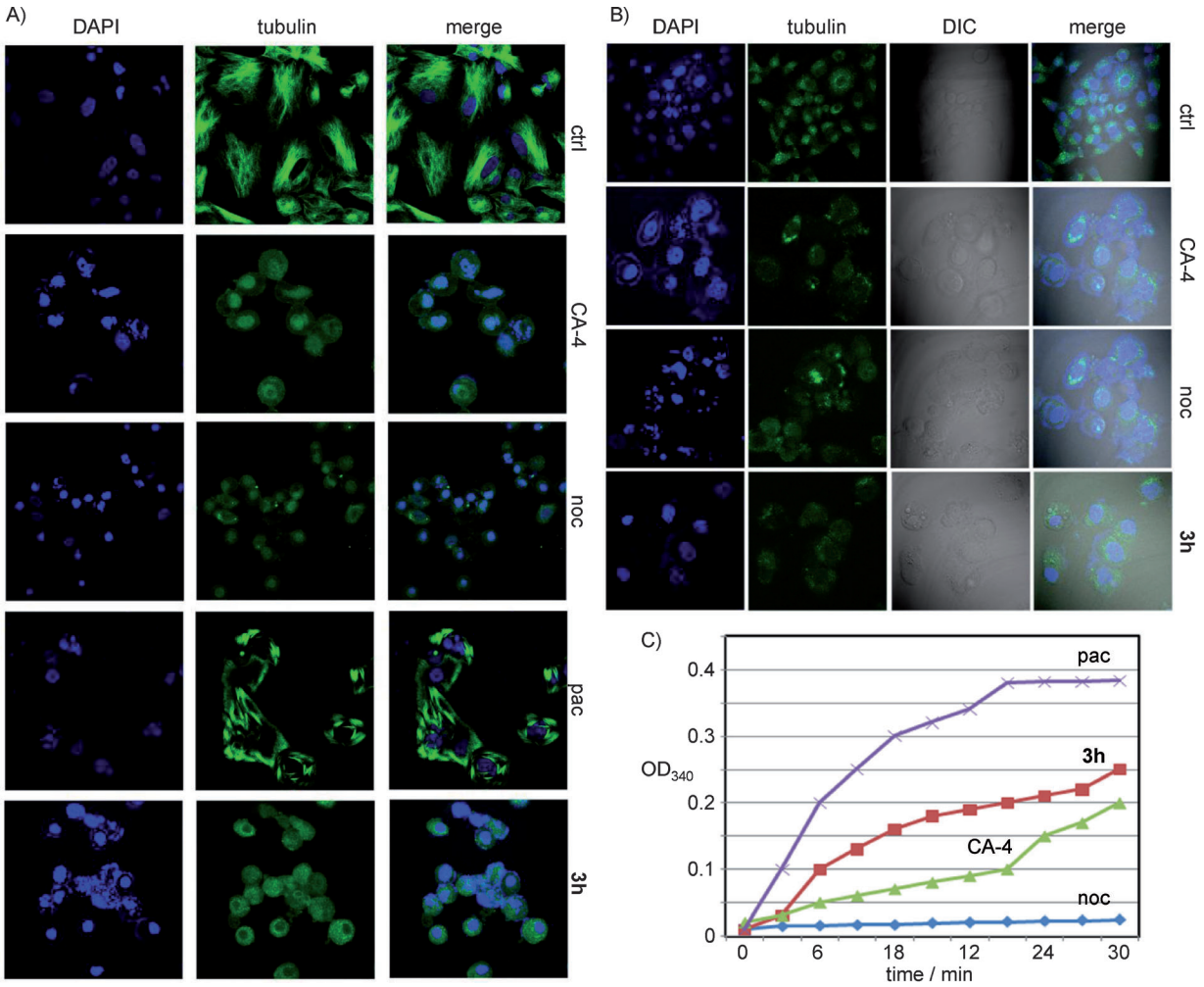

Figure 4. A) Effect of compounds on the microtubule network. A549 cells were treated with CA-4, nocodazole (noc), paclitaxel (pac), and **3h** at 4 μM for 24 h. Microtubule organization can be observed in green in control cells; this was found to be disrupted in cells treated with CA-4, noc, and **3h**. B) Effect of compound **3h** on ectopically expressed tubulin. A549 cells were transfected with tubulin–GFP-expressing plasmid and treated with **3h**, CA-4, and noc at 4 μM for 24 h. Treatment with these compounds resulted in disrupted microtubule patterns relative to untreated control cells. C) Inhibitory activity of compound **3h** on tubulin polymerization. An in vitro high-throughput tubulin polymerization assay was carried out using compounds CA-4, noc, pac, and **3h** at 4 μM. OD readings were taken at λ 340 nM and were used to measure tubulin inhibitory activity.

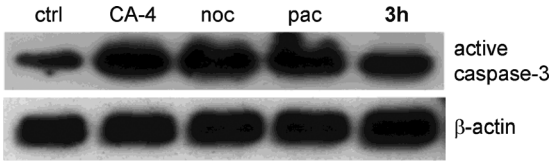

Figure 5. Effect of conjugates on the expression of caspase-3 protein. A549 cells were treated with compounds CA-4, noc, pac, or **3h** for 24 h, and cell lysates were subjected to Western blot for active caspase-3. β-Actin was used as a loading control.

Docking studies

To elucidate the mode of binding to tubulin and consequent microtubule formation, it was considered of interest to examine these fused benzothiazoles (**3a–h**) by directly docking to the colchicine binding site of β-tubulin. AutoDock results suggest that the docking position of the benzothiazole moiety is in the colchicine binding pocket and results in extensive hydrophobic contacts with the binding pocket of the β-chain (Figure 6). The benzothiazole ring is shown to bind to the same position as ring A of colchicine. Amino acids in proximity to the benzothiazole moiety include Cys 241, Leu 242, Ala 250, Leu 255, Val 318, and Ile 378. In addition, hydrophobic contacts were also observed for the phenyl group buried within the region including Ala 80 (from the α-chain), Val 181 (α-chain), Met 259, Ala 316, and the hydrophobic region of Lys 352. The variable moiety of compounds **3a–h** extends into the interface of the α- and β-chains. The naphthyl group of the most active compound (**3h**) is surrounded by Leu 248, the hydrophobic portion of Lys 254, the side chain peptide π-region of Asn 258, Ser 178 and Ala 180 from the α-chain. Compound **3a**, which contains a 4-hydroxy substituent on the phenyl ring, likely forms a hydrogen bond with Lys 254 while the 3-methoxy substituent binds within the hydrophobic region similar to the naphthyl ring of compound **3h**. The thienyl group in compound **3e** is smaller in size than the naphthyl group of com-

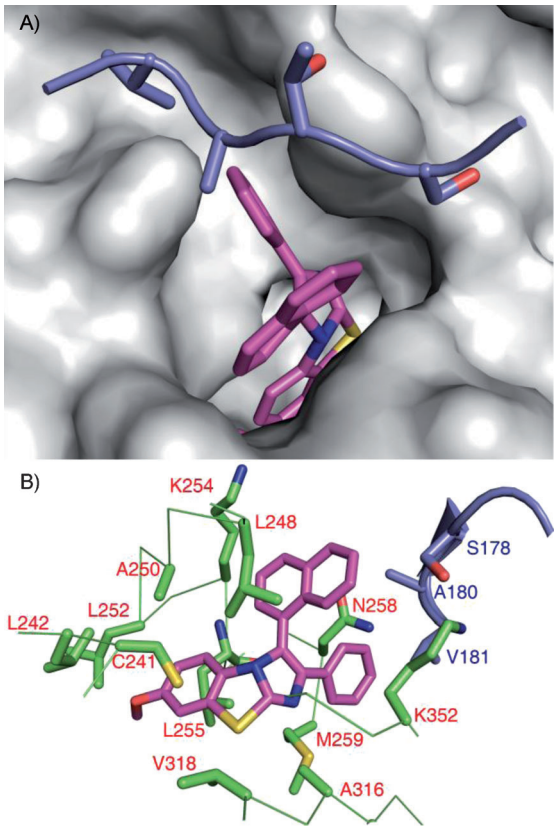

Figure 6. Molecular modeling. A) Binding of compound **3h** to the β-chain (shown as a grey surface) where colchicine is known to bind. The structure in light blue represents the α-chain at Ala 180. Note that common regions of the inhibitors are buried inside the hydrophobic pocket. B) Compound **3h** is shown in magenta, while the β-chain is shown in green and the α-chain in blue. Amino acids surrounding the inhibitor are shown labeled in single-letter code for clarity.

pound **3h** and is therefore buried favorably within the α-/β-chain interface. Compounds **3b**, **3c**, and **3d** are variations of methoxy substitution on the phenyl ring. Dimethoxy-containing compounds **3b** and **3c** have unfavorable interactions with the hydrophobic pocket and do not fit well. Similar interactions were observed with compound **3d**. Although the 4-hydroxy group on phenyl ring is quite favorable, the methoxy group leads to unfavorable interaction with Lys 254, Leu 255, and Asn 258 residues of the β-chain due to the increased steric bulk on the phenyl ring. Both the pyridyl and pyrazinyl rings of compound **3f** and **3g** pack perpendicularly to the naphthyl group, and it is possible that the ring nitrogen groups do not find favorable hydrogen bonding partners, resulting in their insignificance as inhibitors in this series of fused benzothiazoles. Overall, modeling studies carried out not only provide a molecular basis for the mode of binding but also show the specific mode of inhibition of tubulin polymerization.

Conclusions

A series of 3-substituted 2-phenylimidazo[2,1-*b*]benzothiazoles were synthesized using palladium-catalyzed arylation/heteroarylation of 2-arylimidazo[2,1-*b*]benzothiazoles and were evaluated for their anticancer and tubulin polymerization inhibitory potential. These compounds exhibited significant anticancer activity, with GI_{50} values ranging from 0.19 to 83.1 μM. Compound **3h**, containing a naphthyl ring, was the most active amongst this series and showed potent anticancer efficacy against sixty human cancer cell lines with a mean GI_{50} value of 0.88 μM. Moreover, studies showed that compound **3h** arrested cells in the G_2/M phase of the cell cycle, followed by the activation of caspase, as the mechanism of cytotoxicity. A high-throughput tubulin polymerization assay showed that the level of tubulin inhibition for compound **3h** was similar to that of CA-4. The biochemical data presented suggests that compounds **3a** and **3e** arrest the cell cycle in the G1 phase to a greater extent than the G_2/M phase, while the opposite is true of **3h**. The modeling data further confirms that all of these compounds are able to bind to tubulin; however, there may be other mechanistic aspects by which they arrest the cell cycle. Biochemical data of tubulin polymerization inhibition by these fused benzothiazoles corroborates well with the molecular docking studies. The results suggest that these new 3-substituted 2-phenylimidazo[2,1-*b*]benzothiazoles, particularly **3h**, have the potential to be developed as a new class of tubulin polymerization inhibitors for the treatment of cancer.

Experimental Section

Chemistry

All chemicals and reagents were obtained from Aldrich (Sigma–Aldrich, St. Louis, MO, USA), Lancaster (Alfa Aesar, Johnson Matthey Company, Ward Hill, MA, USA), or Spectrochem Pvt. Ltd. (Mumbai, India) and were used without further purification. Reactions were monitored by TLC performed on silica gel glass plates containing 60 GF-254, and visualization was achieved by UV light or iodine indicator. Column chromatography was performed with Merck 60–120 mesh silica gel. ^{1}H spectra were recorded on Bruker UXNMR/XWIN-NMR (300 MHz) or Inova Varian-VXR-unity (400, 500 MHz) instruments. Chemical shifts (δ) are reported in ppm downfield from an internal TMS standard. ESI spectra were recorded on a Micromass Quattro LC using ESI+ software with capillary voltage 3.98 kV and ESI mode positive ion trap detector. High-resolution mass spectra (HRMS) were recorded on a QSTAR XL Hybrid MS–MS mass spectrometer. Melting points were determined with an Electro thermal melting point apparatus, and are uncorrected.

7-Methoxy-2-phenylimidazo[2,1-*b*]benzothiazole (6): A mixture of 6-methoxy-2-aminobenzothiazole (**4**, 1.00 g, 5.55 mmol), 2-bromoacetophenone (**5**, 1.20 g, 6.02 mmol), were dissolved in 10 mL EtOH and stirred for 1 h at reflux. The solution was cooled to room temperature and concentrated under vacuum to remove the EtOH. The resulting crude mass was diluted with H_2O, neutralized with saturated $NaHCO_3$ solution, and extracted with EtOAc to obtain **6** as a white solid. Yield: 1.32 g (84%); mp: 110–111 °C; ^{1}H NMR (300 MHz, $CDCl_3$): $\delta = 8.26$ (s, 1H), 7.88–7.67 (m, 3H), 7.47 (dt, $J =$ 8.3, 0.7 Hz, 1H), 7.42–7.32 (m, 4H), 7.24 (t, $J = 7.4$ Hz, 1H), 3.81 ppm (s, 3H); MS (ESI) *m/z*: 281 $[M+1]^+$.

2-Methoxy-4-(7-methoxy-2-phenylbenzo[*d*]imidazo[2,1-*b*]-[1,3]thiazol-3-yl)phenol (3a): A mixture of 7-methoxy-2-phenylimidazo[2,1-*b*]benzothiazole (**6**, 280 mg, 1 mmol), 4-hydroxy-3-methoxyiodobenzene (**7a**, 250 mg, 1 mmol), $Pd(OAc)_2$ (10 mol%), PPh_3 (290 mg, 0.5 mmol), and Cs_2CO_3 (390 mg, 1.2 mmol) in 1,4-di-

oxane was stirred at reflux for 16 h. Progress of the reaction was monitored by TLC. Following completion of the reaction, the mixture was cooled to room temperature, dioxane was removed under reduced pressure, and the reaction mixture was extracted with EtOAc (3×10 mL). The combined extract was washed with H_2O (1×5 mL) and brine (1×5 mL) and was dried over anhydrous Na_2SO_4. The organic layer was concentrated under reduced pressure, and the crude product was purified by column chromatography using EtOAc/hexane (2:8) as the eluent to afford compound **3a** as a white solid. Yield: 300 mg (74%); mp: 170–171 °C; ^{1}H NMR (500 MHz, $CDCl_3$ + [D_6]DMSO): δ = 9.23 (s, 1H), 8.01 (s, 1H), 7.48–7.40 (m, 2H), 7.32–7.27 (m, 2H), 7.19–7.13 (m, 4H), 6.68–6.62 (m, 2H), 3.78 (s, 3H), 3.45 ppm (s, 3H); MS (ESI) *m/z*: 403 $[M+1]^+$; HRMS (ESI *m/z*) calcd for $C_{24}H_{21}O_3N_2S$: 403.11164, found: 403.11089 $[M+1]^+$; anal. calcd for $C_{23}H_{18}F_3N_2O_3S$: C 68.64, H 4.51, N 6.96, found: C 68.62, H 4.54, N 6.97.

3-(2,4-Dimethoxyphenyl)-7-methoxy-2-phenylbenzo[*d*]imidazo-[2,1-*b*][1,3]thiazole (3b): This compound was prepared according to the method described for compound **3a**, employing compound 7-methoxy-2-phenylimidazo[2,1-*b*]benzothiazole (**6**, 280 mg, 1 mmol) and 2,4-dimethoxyiodobenzene (**7b**, 264 mg, 1 mmol) to obtain pure product **3b** as a white solid. Yield: 330 mg (80%); mp: 165–166 °C; ^{1}H NMR (300 MHz, $CDCl_3$): δ = 7.60–7.56 (m, 2H), 7.27–7.15 (m, 5H), 6.76–6.55 (m, 4H), 3.93 (s, 3H), 3.68 ppm (s, 6H); MS (ESI) *m/z*: 417 $[M+1]^+$; HRMS (ESI *m/z*) calcd for $C_{24}H_{21}O_3N_2S$: 417.12674, found: 417.12556 $[M+1]^+$; anal. calcd for $C_{24}H_{20}N_2O_3S$: C 69.21, H 4.84, N 6.73, found: C 69.24, H 4.82, N 6.74.

3-(2,6-Dimethoxyphenyl)-7-methoxy-2-phenylbenzo[*d*]imidazo-[2,1-*b*][1,3]thiazole (3c): This compound was prepared according to the method described for compound **3a**, employing compound 7-methoxy-2-phenylimidazo[2,1-*b*]benzothiazole (**6**, 280 mg, 1 mmol) and 2,6-dimethoxyiodobenzene (**7c**, 264 mg,1 mmol) to obtain pure product **3c** as a white solid. Yield: 340 mg (81%); mp: 175–176 °C; ^{1}H NMR (500 MHz, $CDCl_3$): δ = 7.54–7.52 (m, 2H), 7.46–7.42 (m, 1H), 7.19–7.16 (m, 2H), 7.12–7.08 (m, 2H), 6.66–6.61 (m, 4H), 3.79 (s, 3H), 3.60 ppm (s, 6H); ^{13}C NMR (75 MHz, $CDCl_3$): δ = 156.5, 134.6, 133.6, 131.9, 130.3, 128.1, 126.4, 113.6, 112.8, 108.2, 105.1, 99.1, 55.7, 55.5, 55.4 ppm; MS (ESI) *m/z*: 417 $[M+1]^+$; HRMS (ESI *m/z*) calcd for $C_{24}H_{21}O_3N_2S$: 417.12674, found: 417.12638 $[M+1]^+$; anal. calcd for $C_{24}H_{20}N_2O_3S$: C 69.21, H 4.84, N 6.73, found: C 69.19, H 4.85, N 6.76.

7-Methoxy-2-phenyl-3-(3,4,5-trimethoxyphenyl)benzo[*d*]imidazo-[2,1-*b*][1,3]thiazole (3d): This compound was prepared according to the method described for compound **3a**, employing compound 7-methoxy-2-phenylimidazo[2,1-*b*]benzothiazole (**6**, 280 mg, 1 mmol) and 3,4,5-trimethoxyiodobenzene (**7d**, 294 mg,1 mmol) to obtain pure product **3d** as a white solid. Yield: 360 mg (80%); mp: 170–171 °C; ^{1}H NMR (300 MHz, $CDCl_3$): δ = 7.61–7.59 (m, 2H), 7.29–7.24 (m, 2H), 7.21–7.17 (m, 2H), 6.80 (s, 1H), 6.77–6.74 (m, 3H), 4.00 (s, 3H), 3.83 (s, 3H), 3.81 ppm (s, 6H); ^{13}C NMR (75 MHz, $CDCl_3$): δ = 156.7, 153.8, 131.7, 128.2, 126.8, 126.5, 125.4, 123.9, 113.9, 112.9, 108.6, 107.9, 104.5, 61.1, 60.9, 56.2, 55.8 ppm; MS (ESI) *m/z*: 447 $[M+1]^+$; HRMS (ESI *m/z*) calcd for $C_{25}H_{23}O_4N_2S$: 447.13730, found: 447.13729 $[M+1]^+$; anal. calcd for $C_{25}H_{22}N_2O_4S$: C 67.25, H 4.97, N 6.27, found: C 67.27, H 4.93, N 6.24.

7-Methoxy-2-phenyl-3-(3-thienyl)benzo[*d*]imidazo[2,1-*b*]-[1,3]thiazole (3e): This compound was prepared according to the method described for compound **3a**, employing compound 7-methoxy-2-phenylimidazo[2,1-*b*]benzothiazole (**6**, 280 mg, 1 mmol) and 3-iodothiophene (**7e**, 210 mg,1 mmol) to obtain pure product **3e** as a white solid. Yield: 300 mg (83%); mp 168–169 °C; ^{1}H NMR (300 MHz, $CDCl_3$): δ = 7.51–7.48 (m, 4H), 7.27–7.13 (m, 5H), 6.80–6.77 (d, *J* = 9.0 Hz, 1H), 6.72–6.70 (d, *J* = 9.0 Hz, 1H), 3.81 ppm (s, 3H); MS (ESI) *m/z*: 363 $[M+1]^+$; HRMS (ESI *m/z*) calcd for $C_{20}H_{15}N_2OS_2$: 363.06258, found: 363.05778 $[M+1]^+$; anal. calcd for $C_{20}H_{14}N_2OS_2$: C 66.27, H 3.89, N 7.73, found: C 66.29, H 3.93, N 7.72.

7-Methoxy-2-phenyl-3-(3-pyridyl)benzo[*d*]imidazo[2,1-*b*]-[1,3]thiazole (3f): This compound was prepared according to the method described for compound **3a**, employing compound 7-methoxy-2-phenylimidazo[2,1-*b*]benzothiazole (**6**, 280 mg, 1 mmol) and 3-iodopyridine (**7f**, 205 mg,1 mmol) to obtain pure product **3f** as a white solid. Yield: 270 mg (76%); mp: 166–167 °C; ^{1}H NMR (300 MHz, $CDCl_3$ + [D_6]DMSO): δ = 8.78–8.76 (d, *J* = 5.0 Hz, 1H), 8.74 (s, 1H), 7.92–7.91 (d, *J* = 8.0 Hz, 1H), 7.56–7.54 (m, 1H), 7.43–7.41 (m, 2H), 7.33 (s, 1H), 7.23–7.15 (m. 3H), 6.76–6.71 (m, 2H), 3.81 ppm (s, 3H); ^{13}C NMR (75 MHz, $CDCl_3$): δ = 151.7, 150.3, 138.7, 128.9, 127.2, 127.1, 123.9, 113.5, 112.9, 108.8, 55.8 ppm; MS (ESI) *m/z*: 358 $[M+1]^+$; HRMS (ESI *m/z*) calcd for $C_{21}H_{16}ON_3S$: 358.10086, found: 358.09944 $[M+1]^+$; anal. calcd for $C_{21}H_{15}N_3OS$: C 70.57, H 4.23, N 11.76, found: C 70.60, H 4.19, N 11.73.

7-Methoxy-2-phenyl-3-(2-pyrazinyl)benzo[*d*]imidazo[2,1-*b*]-[1,3]thiazole (3g): This compound was prepared according to the method described for compound **3a**, employing compound 7-methoxy-2-phenylimidazo[2,1-*b*]benzothiazole (**6**, 280 mg, 1 mmol) and 2-iodopyrazine (**7g**, 206 mg,1 mmol) to obtain pure product **3g** as a white solid. Yield: 300 mg (83%); mp: 169–170 °C; ^{1}H NMR (500 MHz, $CDCl_3$ + [D_6]DMSO): δ = 8.63 (d, *J* = 7.5 Hz, 1H), 8.43 (s, 1H), 7.45 (d, *J* = 7.5 Hz, 1H), 7.38–7.33 (m, 2H), 7.30–7.20 (m, 3H), 7.18 (s, 1H), 6.89–6.78 (m, 2H), 3.79 ppm (s, 3H) MS (ESI) *m/z*: 359 $[M+1]^+$; HRMS (ESI *m/z*) calcd for $C_{20}H_{15}N_4OS$: 359.09666, found: 359.09586 $[M+1]^+$; anal. calcd for $C_{20}H_{14}N_4OS$: C 67.02, H 3.94, N 15.63, found: C 67.00, H 3.96, N 15.65.

7-Methoxy-3-(2-naphthyl)-2-phenylbenzo[*d*]imidazo[2,1-*b*]-[1,3]thiazole (3h): This compound was prepared according to the method described for compound **3a**, employing compound 7-methoxy 2-phenylimidazo[2,1-*b*]benzothiazole (**6**, 280 mg, 1 mmol) and 1-iodonaphthalene (**7h**, 254 mg,1 mmol) to obtain pure product **3h** as a white solid. Yield: 360 mg (88%); mp: 170–171 °C; ^{1}H NMR (500 MHz, $CDCl_3$): δ = 7.85 (s, 1H), 7.82–7.80 (m, 2H), 7.66–7.59 (m, 1H), 7.55–7.51 (m, 1H), 7.48–7.45 (m, 2H), 7.39–7.36 (m, 3H), 7.26–7.23 (m, 1H), 7.19–7.18 (m. 1H), 7.14–7.07 (m, 2H), 6.97–6.95 (m, 1H), 3.31 ppm (s, 3H)); ^{13}C NMR (75 MHz, [D_6]DMSO): δ = 154.1, 148.8, 143.9, 143.4, 133.7, 132.8, 132.1, 132.0, 129.8, 129.1, 128.2, 128.1, 128.0, 127.2, 126.8, 126.2, 123.2, 121.6, 120.4, 101.2, 56.1, 55.6 ppm; MS (ESI) *m/z*: 407 $[M+1]^+$; HRMS (ESI *m/z*) calcd for $C_{26}H_{19}ON_2S$: 407.12069, found: 407.12126 $[M+1]^+$; anal. calcd for $C_{26}H_{18}N_2OS$: C 76.82, H 4.46, N 6.89, found: C 76.80, H 4.49, N 6.86.

Biology

Cell culture: The A549 human lung cancer cell line was purchased from American Type Culture Collection and maintained in Dulbecco's modified Eagle's medium (DMEM) (Invitrogen), supplemented with 2 mM glutamax (Invitrogen), 10% fetal calf serum, 100 U mL^{-1} penicillin and 100 mg mL^{-1} streptomycin sulfate (Sigma). The cell line was maintained at 37 °C in a humidified atmosphere containing 5% CO_2.

MTT assay: Cell viability was assessed using an MTT mitochondrial function assay, based on the ability of viable cells to reduce MTT to insoluble formazan crystals by mitochondrial dehydrogenase. A549 cells were seeded in a 96-well plate at a density of 10000

cells per well. Following overnight incubation, cells were treated with compounds **3a**–**h** and CA-4 at 4 μM and were incubated for 24 h. The medium was then discarded and replaced with 10 μL MTT dye. Plates were incubated at 37 °C for 2 h. The resulting formazan crystals were solubilized in 100 μL extraction buffer. The optical density (OD) was read at λ 570 nm with a microplate reader (Multi-mode Varioskan Instrument, Thermo Scientific).

Immunofluorescence assay: A549 cells were seeded on cover slips and treated with 4 μM **3h**, noc, CA-4, or pac for 24 h. After treatment, cover slips were fixed with a paraformaldehyde solution (4% in 1× PBS) for 20 min at room temperature. Cell permeabilization was achieved by administration of a Triton X-100 solution (0.2% in 1× PBS) for 5 min. The cover slips were left in 100% MeOH overnight at 4 °C. Subsequently, cover slips were blocked with a 1% BSA solution for 60 min, then incubated with anti α-tubulin antibody (1:100) at room temperature for 2 h. The slides were washed three times for 5 min each with PBST. Next, cover slips were incubated with a FITC-conjugated anti-rabbit secondary antibody (Jackson Immuno Research Laboratories Inc., Pennsylvania, USA) for 1 h then were washed three times with PBST solution and mounted with DAPI/PI solution. Finally, cells were observed under a confocal microscope (Olympus FV1000). Collected images were processed with the support of Flow View version 1.7c software [DakoCytomation (Beckman Coulter, Brea, CA, USA)].

Tubulin transfection studies: Human A549 cells were seeded on cover slips. The tubulin-expressing plasmid construct was transiently transfected with lipofectamine 2000. After 24 h, the A549 cells were treated with compound **3h**, CA-4, noc, or pac at 4 μM for 24 h. Cells were then examined using confocal microscopy and images were collected.

Tubulin polymerization assay: A tubulin polymerization assay was conducted using cytoskeleton kit BK-004 (Lab-pro Company, Denver, CO, USA). Compounds **3h**, CA-4, noc, and pac were incubated with tubulin (100 μL) as provided in the kit, and readings were taken for 30 min to 1 h. The OD values at λ 340 nm were measured, and inhibition graphs were plotted (MS Office Excel 2007).

Cell-cycle analysis: 5×10^5 A549 cells were seeded in 60 mm dishes and were allowed to grow for 24 h. Compounds **3a**–**h** or CA-4 (positive control) at were added to the culture media to a final concentration of 4 μM, and the cells were incubated for an additional 24 h. Cells were harvested with Trypsin-EDTA, fixed with ice-cold 70% EtOH at 4 °C for 30 min, washed with PBS, and incubated with 1 mg mL^{-1} RNAse solution (Sigma) at 37 °C for 30 min. Cells were collected by centrifugation at 2000 rpm for 5 min and were further stained with 250 mL DNA staining solution [10 mg propidium iodide (PI), 0.1 mg trisodium citrate, and 0.03 mL Triton X-100, dissolved in 100 mL sterile water at room temperature for 30 min in the dark]. The DNA contents of 20000 events were measured using a DakoCytomation flow cytometer (Beckman Coulter, Brea, CA, USA). Histograms were analyzed using Summit Software.

Protein extraction and Western blot analysis: A549 human lung cancer cells were seeded in 60 mm dishes and were allowed to grow to attain 80% confluency for 24 h. Compounds (**3h**, CA-4, noc, or pac) were added to the culture media for a final concentration of 4 μM, and the cells were incubated with compounds for 24 h. After 24 h, total cell lysates from cultured A549 cells were obtained by lysing the cells in ice-cold RIPA buffer (1× PBS, 1% NP-40, 0.5% sodium deoxycholate, and 0.1% SDS) containing 100 mg mL^{-1} PMSF, 5 mg mL^{-1} aprotinin, 5 mg mL^{-1} leupeptin, 5 mg mL^{-1} pepstatin, and 100 mg mL^{-1} NaF. After centrifugation at 12000 rpm (8064 *g*) for 10 min, protein in the supernatant was quantified by the Bradford method (BioRad) using a Multimode VarioSkan instrument (Thermo Scientific); 50 mg protein per lane was loaded on a 12% SDS-polyacrylamide gel. After electrophoresis, the protein was transferred to a polyvinylidine difluoride (PVDF) membrane (Amersham Biosciences). The membrane was blocked at room temperature for 2 h in TBS containing 0.1% Tween 20 (TBST) with 5% blocking powder (Santa Cruz Biotechnology). The membrane was washed with TBST for 5 min, then primary antibody was added and incubated at 4 °C overnight. Active caspase-3 and β-actin were purchased from Imgenex Corporation (San Diego, CA, USA). Membranes were washed three times with TBST for 15 min, and the blots were visualized with chemiluminescence reagent (Thermo Scientific). X-ray films were developed and fixed using solutions from Kodak.

Molecular modeling

Tubulin bound to colchicine (PDB code: 3E22) was selected as the receptor for docking simulations. After removing the ligand and solvent molecules, hydrogen atoms and Kollman charges were added to each protein atom. Coordinates for each compound were obtained from Chemdraw11 followed by MM2 energy minimization. Docking was carried out by AutoDock4 in the colchicine binding pocket.[50–52] Grid map in AutoDock was used to define the interaction of protein and ligand in the binding pocket. The grid map was used with 60 points in each *x*, *y*, and *z* direction, equally spaced at 0.375 Å. Docking was performed using the Lamarckian genetic algorithm.[53] Each docking experiment was performed 100 times, yielding 100 docked conformations. Parameters used for the docking were as follows: population size of 150; random starting position and conformation; maximal mutation of 2 Å translation and 50 degrees rotation; elitism of 1; mutation rate of 0.02 and crossover rate of 0.8; and local search rate of 0.06. Simulations were performed with a maximum of 1.5 million energy evaluations and a maximum of 50000 generations. Final docked conformations were clustered using a tolerance of 1 Å root mean square deviation (RMSD). The best model was chosen based on the most favorable stabilization energy.

Acknowledgements

The authors are thankful to the Council of Scientific and Industrial Research (CSIR), India (F.S. and A.V.) and the University Grants Commission (UCG), New Delhi, India (Y.V.V.S. and C.K.) for the award of research fellowships.

Keywords: antitumor agents · benzothiazoles · caspases · molecular modeling · tubulin

[1] M. A. Jordan, J. A. Hadfield, N. J. Lawrence, A. T. McGown, *Med. Res. Rev.* **1998**, *18*, 259–296.
[2] Y. Zhao, W. S. Fang, K. Pors, *Expert Opin. Ther. Pat.* **2009**, *19*, 607–622.
[3] R. O. Carlson, *Expert Opin. Invest. Drugs* **2008**, *17*, 707–722.
[4] E. Pasquier, M. Kavallaris, *IUBMB Life* **2008**, *60*, 165–170.
[5] M. Kavallaris, *Nat. Rev. Cancer* **2010**, *10*, 194–204.
[6] a) G. R. Pettit, S. B. Singh, E. Hamel, C. M. Lin, D. S. Alberts, D. Garcia-Kendall, *Experientia* **1989**, *45*, 209–211; b) A. Cirla, J. Mann, *Nat. Prod. Rep.* **2003**, *20*, 558–564; c) Y. Shan, J. Zhang, Z. Liu, M. Wang, Y. Dong, *Curr. Med. Chem.* **2011**, *18*, 523–538.

[7] G. J. Rustin, G. Shreeves, P. D. Nathan, A. Gaya, T. S. Ganesan, D. Wang, J. Boxall, L. Poupard, D. J. Chaplin, M. R. Stratford, J. Balkissoon, M. Zweifel, *Br. J. Cancer* **2010**, *102*, 1355 – 1360.
[8] a) J. K. Buolamwini, *Curr. Opin. Chem. Biol.* **1999**, *3*, 500 – 509; b) X. Ding, Z. Zhang, S. Li, A. Wang, *Oncol. Res.* **2011**, *19*, 303 – 309.
[9] D. W. Siemann, D. J. Chaplin, P. A. Walicke, *Expert Opin. Investig. Drugs* **2009**, *18*, 189 – 197.
[10] a) M. K. Gurjar, R. D. Wakharkar, A. T. Singh, M. Jaggi, H. B. Borate, P. D. Shinde, R. Verma, P. Rajendran, S. Dutt, G. Singh, V. K. Sanna, M. K. Singh, S. K. Srivastava, V. A. Mahajan, V. H. Jadhav, K. Dutta, K. Krishnan, A. Chaudhary, S. K. Agarwal, R. Mukherjee, A. C. Burman, *J. Med. Chem.* **2007**, *50*, 1744 – 1753; b) Y. W. Li, J. Liu, N. Liu, D. Shi, X. T. Zhou, J. G. Lv, J. Zhu, C. H. Zheng, Y. J. Zhou, *Bioorg. Med. Chem.* **2011**, *19*, 3579 – 3584; c) K. Ohsumi, T. Hatanaka, K. Fujita, R. Nakagawa, Y. Fukuda, Y. Niher, Y. Suga, Y. Morinaga, Y. Akiyama, T. Tsuji, *Bioorg. Med. Chem. Lett.* **1998**, *8*, 3153 – 3158; d) G. C. Tron, T. Pirali, G. Sorba, F. Pagliai, S. Busacca, A. A. Genazzani, *J. Med. Chem.* **2006**, *49*, 3033 – 3044; e) K. Odlo, J. Hentzen, J. F. dit Chabert, S. Ducki, O. A. Gani, I. Sylte, M. Skrede, V. A. Florenes, T. V. Hansen, *Bioorg. Med. Chem.* **2008**, *16*, 4829 – 4838; f) R. Romagnoli, P. G. Baraldi, O. Cruz-Lopez, C. Lopez Cara, M. D. Carrion, A. Brancale, E. Hamel, L. Chen, R. Bortolozzi, G. Basso, G. Viola, *J. Med. Chem.* **2010**, *53*, 4248 – 4258; g) Q. Zhang, Y. Peng, X. I. Wang, S. M. Keenan, S. Arora, W. J. Welsh, *J. Med. Chem.* **2007**, *50*, 749 – 754.
[11] G. C. Porretta, F. Cerreto, R. Fioravanti, M. Scalzo, M. Fischetti, F. Riccardi, A. Capezzone de Joannon, G. de Feo, G. Mazzanti, L. Tolu, *Farmaco Sci.* **1988**, *43*, 15 – 28.
[12] V. Zuliani, M. Fantini, A. Nigam, J. P. Stables, M. K. Patel, M. Rivara, *Bioorg. Med. Chem.* **2010**, *18*, 7957 – 7965.
[13] M. Fantini, M. Rivara, V. Zuliani, C. L. Kalmar, F. Vacondio, C. Silva, A. R. Baheti, N. Singh, E. C. Merrick, R. S. Katari, G. Cocconcelli, C. Ghiron, M. K. Patel, *Bioorg. Med. Chem.* **2009**, *17*, 3642 – 3648.
[14] a) T. N. Tuyen, K. S. Sin, H. P. Kim, H. Park, *Arch. Pharmacal Res.* **2005**, *28*, 1013 – 1018; b) I. K. Khanna, Y. Yu, R. M. Huff, R. M. Weier, X. Xu, F. J. Koszyk, P. W. Collins, J. N. Cogburn, P. C. Isakson, C. M. Koboldt, J. L. Masferrer, W. E. Perkins, K. Seibert, A. W. Veenhuizen, J. Yuan, D. C. Yang, Y. Y. Zhang, *J. Med. Chem.* **2000**, *43*, 3168 – 3185.
[15] C. W. Plummer, P. E. Finke, S. G. Mills, J. Wang, X. Tong, G. A. Doss, T. M. Fong, J. Z. Lao, M. T. Schaeffer, J. Chen, C. P. Shen, D. S. Stribling, L. P. Shearman, A. M. Strack, L. H. Van der Ploeg, *Bioorg. Med. Chem. Lett.* **2005**, *15*, 1441 – 1446.
[16] F. Bellina, S. Cauteruccio, A. Di Fiore, R. Rossi, *Eur. J. Org. Chem.* **2008**, 5436 – 5455.
[17] K. Bonezzi, G. Taraboletti, P. Borsotti, F. Bellina, R. Rossi, R. Giavazzi, *J. Med. Chem.* **2009**, *52*, 7906 – 7910.
[18] a) R. Schobert, B. Biersack, A. Dietrich, K. Effenberger, S. Knauer, T. Mueller, *J. Med. Chem.* **2010**, *53*, 6595 – 7602; b) W. T. Li, D. R. Hwang, J. S. Song, C. P. Chen, J. J. Chuu, C. B. Hu, H. L. Lin, C. L. Huang, C. Y. Huang, H. Y. Tseng, C. C. Lin, T. W. Chen, C. H. Lin, H. S. Wang, C. C. Shen, C. M. Chang, Y. S. Chao, C. T. Chen, *J. Med. Chem.* **2010**, *53*, 2409 – 2417.
[19] K. Chegaev, L. Lazzarato, P. Tosco, C. Cena, E. Marini, B. Rolando, P. A. Carrupt, R. Fruttero, A. Gasco, *J. Med. Chem.* **2007**, *50*, 1449 – 1457.
[20] L. Navidpour, H. Shadnia, H. Shafaroodi, M. Amini, A. R. Dehpour, A. Shafiee, *Bioorg. Med. Chem.* **2007**, *15*, 1976 – 1982.
[21] C. Almansa, J. Alfón, A. F. de Arriba, F. L. Cavalcanti, I. Escamilla, L. A. Gómez, A. Miralles, R. Soliva, J. Bartrolí, E. Carceller, M. Merlos, J. García-Rafanell, *J. Med. Chem.* **2003**, *46*, 3463 – 3475.
[22] F. Bellina, S. Cauteruccio, S. Monti, R. Rossi, *Bioorg. Med. Chem. Lett.* **2006**, *16*, 5757 – 5762.
[23] L. Wang, K. W. Woods, Q. Li, K. J. Barr, R. W. McCroskey, S. M. Hannick, L. Gherke, R. B. Credo, Y. H. Hui, K. Marsh, R. Warner, J. Y. Lee, N. Zielinski-Mozng, D. Frost, S. H. Rosenberg, H. L. Sham, *J. Med. Chem.* **2002**, *45*, 1697 – 1711.
[24] a) J. Chen, Z. Wang, C. M. Li, Y. Lu, P. K. Vaddady, B. Meibohm, J. T. Dalton, D. D. Miller, W. J. Li, *J. Med. Chem.* **2010**, *53*, 7414 – 7427; b) J. Chen, C. M. Li, J. Wang, S. Ahn, Z. Wang, Y. Lu, J. T. Dalton, D. D. Miller, W. Li, *Bioorg. Med. Chem.* **2011**, *19*, 4782 – 4795.
[25] V. Trapani, V. Patel, C. O. Leong, H. P. Ciolino, G. C. Yeh, C. Hose, J. B. Trepel, M. F. Stevens, E. A. Sausville, A. I. Loaiza-Pérez, *Br. J. Cancer* **2003**, *88*, 599 – 605.
[26] D. F. Shi, T. D. Bradshaw, S. Wrigley, C. J. McCall, P. Lelieveld, I. Fichtner, M. F. Stevens, *J. Med. Chem.* **1996**, *39*, 3375 – 3384.
[27] T. D. Bradshaw, A. D. Westwell, *Curr. Med. Chem.* **2004**, *11*, 1009 – 1021.
[28] D. Vullo, M. Franchi, E. Gallori, J. Antel, A. Scozzafava, C. T. Supuran, *J. Med. Chem.* **2004**, *47*, 1272 – 1279.
[29] A. Kamal, Y. V. V. Srikanth, M. N. A. Khan, M. Ashraf, M. K. Reddy, F. Sultana, T. Kaur, G. Chashoo, N. Suri, I. Sehar, Z. A. Wani, A. Saxena, P. R. Sharma, S. Bhushan, D. M. Mondhe, A. K. Saxena, *Bioorg. Med. Chem.* **2011**, *19*, 7136 – 7150.
[30] a) T. H. Al-Tel, R. A. Al-Qawasmeh, R. Zaarour, *Eur. J. Med. Chem.* **2011**, *46*, 1874; b) M. Palkar, M. Noolvi, R. Sankangoud, V. Maddi, A. Gadad, L. V. Nargund, *Arch. Pharm.* **2010**, *343*, 353 – 359.
[31] A. N. el-Shorbagi, S. Sakai, M. A. el-Gendy, N. Omar, H. H. Farag, *Chem. Pharm. Bull.* **1989**, *37*, 2971 – 2975.
[32] T. Mase, H. Arima, K. Tomioka, T. Yamada, K. Murase, *J. Med. Chem.* **1986**, *29*, 386 – 394.
[33] I. R. Ager, A. C. Barnes, G. W. Danswan, P. W. Hairsine, D. P. Kay, P. D. Kennewell, S. S. Matharu, P. Miller, P. Robson, D. A. Rowlands, *J. Med. Chem.* **1988**, *31*, 1098 – 1115.
[34] K. Srimanth, V. R. Rao, D. R. Krishna, *Arzneimittelforschung* **2002**, *52*, 388 – 392.
[35] G. Trapani, M. Franco, A. Latrofa, A. Reho, G. Liso, *Eur. J. Pharm. Sci.* **2001**, *14*, 209 – 216.
[36] N. Amino, Y. Ideyama, M. Yamano, S. Kuromitsu, K. Tajinda, K. Samizu, A. Matsuhisa, M. Kudoh, M. Shibasaki, *Cancer Lett.* **2006**, *238*, 119 – 127.
[37] D. Alagille, H. DaCosta, R. M. Baldwin, G. D. Tamagnan, *Bioorg. Med. Chem. Lett.* **2011**, *21*, 2966 – 2968.
[38] M. S. Christodoulou, F. Colombo, D. Passarella, G. Ieronimo, V. Zuco, M. De Cesare, F. Zunino, *Bioorg. Med. Chem.* **2011**, *19*, 1649 – 1657.
[39] R. M. Kumbhare, K. V. Kumar, M. J. Ramaiah, T. Dadmal, S. N. Pushpavalli, D. Mukhopadhyay, B. Divya, T. A. Devi, U. Kosurkar, M. Pal-Bhadra, *Eur. J. Med. Chem.* **2011**, *46*, 4258 – 4266.
[40] A. Kamal, M. N. A. Khan, Y. V. V. Srikanth, K. S. Reddy, A. Juvekar, S. Sen, N. Kurian, S. Zingde, *Bioorg. Med. Chem.* **2008**, *16*, 7804 – 7810.
[41] A. Kamal, V. Tekumalla, A. Krishnan, M. Pal-Bhadra, U. Bhadra, *ChemMedChem* **2008**, *3*, 794 – 802.
[42] A. Kamal, Y. V. V. Srikanth, T. B. Shaik, M. N. A. Khan, M. Ashraf, M. K. Reddy, K. A. Kumar, S. V. Kalivendi, *Med. Chem. Commun.* **2011**, *2*, 819 – 823.
[43] A. Kamal, D. Dastagiri, M. J. Ramaiah, J. S. Reddy, E. V. Bharathi, C. Srinivas, D. Pal, M. Pal-Bhadra, *ChemMedChem* **2010**, *5*, 1937 – 1947.
[44] A. Kamal, Y. V. V. Srikanth, M. N. A. Khan, T. B. Shaik, M. Ashraf, *Bioorg. Med. Chem. Lett.* **2010**, *20*, 5229 – 5231.
[45] a) F. Bellina, S. Cauteruccio, L. Mannina, R. Rossi, S. Viel, *J. Org. Chem.* **2005**, *70*, 3997 – 4005; b) F. Bellina, S. Cauteruccio, R. Rossi, *J. Org. Chem.* **2007**, *72*, 8543 – 8546; c) F. Bellina, S. Cauteruccio, A. Di Fiore, C. Marchetti, R. Rossi, *Tetrahedron* **2008**, *64*, 6060 – 6072.
[46] C. Kanthou, O. Greco, A. Stratford, I. Cook, R. Knight, O. Benzakour, G. Tozer, *Am. J. Pathol.* **2004**, *165*, 1401 – 1411.
[47] L. H. Zhang, L. Wu, H. K. Raymon, R. S. Chen, L. Corral, M. A. Shirley, R. K. Narla, J. Gamez, G. W. Muller, D. I. Stirling, B. J. Bartlett, P. H. Schafer, F. Payvandi, *Cancer Res.* **2006**, *66*, 951 – 959.
[48] S. Kumar, *Cell Death Differ.* **2007**, *14*, 32 – 43.
[49] N. A. Thornberry, *Chem. Biol.* **1998**, *5*, R97 – 103.
[50] AutoDock version 4.0, http://www.scripps.edu/mb/olson/doc/autodock/.
[51] R. B. Ravelli, B. Gigant, P. A. Curmi, I. Jourdain, S. Lachkar, A. Sobel, M. Knossow, *Nature* **2004**, *428*, 198 – 202.
[52] M. A. Reddy, N. Jain, D. Yada, C. Kishor, J. R. Vangala, R. Surendra, A. Addlagatta, S. V. Kalivendi, B. Sreedhar, *J. Med. Chem.* **2011**, *54*, 6751 – 6760.
[53] G. M. Morris, D. S. Goodsell, R. S. Halliday, R. Huey, W. E. Hart, R. K. Belew, A. J. Olson, *J. Comput. Chem.* **1998**, *19*, 1639 – 1662.

Received: November 3, 2011
Revised: December 7, 2011
Published online on January 12, 2012

